Fast chatter stability prediction for variable helix milling tools

Journal Title
XX(X):1–??

DOI: 10.1177/ToBeAssigned
www.sagepub.com/
SAGE

Neil D Sims[1]

Abstract

Regenerative chatter is a well-known form of self-excited vibration that limits the productivity of machining operations, in particular for milling. Variable helix tools have been previously proposed as a means of avoiding regenerative chatter, and although recent work has analysed the stability of such tools there has not always been a strong agreement with experimentally observed behaviour. Furthermore, the analysis of variable helix tool stability can be tedious and numerically slow, compared to standard tools. Consequently it has been difficult to gain insight into the potential advantages of variable helix tools. The present work attempts to address these issues, by first developing an efficient approach to variable helix tool stability based upon the Laplace transform. Then, this new analysis method is used to demonstrate the importance of multi-frequency effects and nonlinear cutting stiffness. The work suggests that whilst variable-helix tools can have more operating regions that are stable, un-modelled behaviour (such as nonlinearity and multi-frequency effects) can have a critical influence on the accuracy of model predictions.

Keywords

milling, machining, machining dynamics, milling dynamics, regenerative chatter, bode diagram, comb filter

[1]The University of Sheffield, UK

Corresponding author:
Neil D Sims, Department of Mechanical Engineering, The University of Sheffield, Mappin Street, Sheffield, S1 3JD, UK
Email: n.sims@sheffield.ac.uk

Nomenclature

a	coordinate along tool axis (m)
a_{xx}	direction coefficient
a_{xy}	direction coefficient
a_{yx}	direction coefficient
a_{yy}	direction coefficient
b	depth of cut in coordinate direction a (m)
b_c	critical depth of cut (m)
$f_{t,j}$	tangential cutting force for tool j (N)
$f_{r,j}$	radial cutting force for tool j (N)
f_x	force in x-direction (N)
f_y	force in y-direction (N)
g	unit step function
h	chip thickness (m)
j	tooth number
r_t	tool radius (m)
s_t	feed per tooth (m)
t	time (s)
$v_{j,0}$	previous instantaneous chip thickness for tool j (m)
v_j	current instantaneous chip thickness for tool j (m)
x	tool position (m)
y	tool position (m)
G_c	cutting gain (N/m)
G_d	delay transfer function
G_{tot}	total transfer function
G_x	transfer function in x-direction
K_t	tangential cutting force coefficient (N/m^2
K_r	radial cutting force coefficient (N/m^2)
N_t	number of cutting teeth
α	helix angle (rad)
α_{xx}	time-averaged direction coefficient
α_{xy}	time-averaged direction coefficient
α_{yx}	time-averaged direction coefficient
α_{yy}	time-averaged direction coefficient
β	variable helix delay coefficient (s/m)
ϕ_{st}	angle of tool entry into workpiece (rad)
ϕ_{ex}	angle of tool departure from workpiece (rad)
ϕ_j	angular coordinate of tool j (rad)
τ	time delay (s)
τ_r	delay per tool revolution (s)

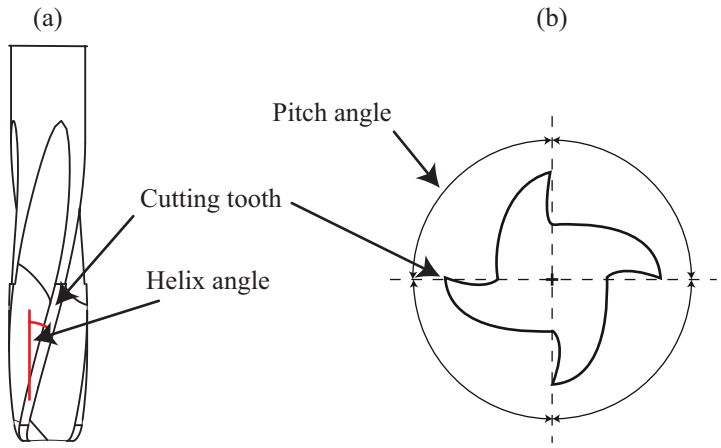

Figure 1. Milling tool geometry. (a) side view; (b) end view of the tip of the cutting tool

1 Introduction

The productivity of metal removal operations is often limited by the onset of regenerative chatter[1]. Consequently, there has been a great deal of research to try to understand, predict, and avoid, the onset of this unstable self-excited vibration. In recent years, techniques proposed to avoid chatter have included: active vibration control[2], tuned mass damping,[3;4] variations in machine spindle speed[5], and variable-helix tools. The present study is concerned with variable helix tools, which are introduced with reference to Fig. 1.

For regular tools, the time delay between successive teeth is constant and fixed, because the helix and pitch angles are the same for every tooth. For variable pitch tools the time delay can be different for each tooth due to changes in the pitch angle. However, for variable helix tools the time delay can change along the axis of the tool, due to changes or differences in the tooth helix angle. These changes in the time delays within the system are the key to potentially enhanced stability from the more complex tools geometries. However, in practice other factors (such as the ability to remove swarth from the flutes of the tool) are also important in evaluating the performance of the tool. The background literature concerning variable helix tools will now be briefly discussed.

One of the first studies to propose variable helix tools was the work of Stone[6] in 1970. Whilst variable pitch tools have received a great deal of attention (e.g. Budak[7]), variable helix tools been more difficult to understand and exploit in practice. A detailed methodology for analysing the stability of variable helix tools was described by Sims *et al.*[8]. The modelling approach was partly motivated by the work of Turner *et al.*[9], who developed an averaging-based approach to modelling variable-helix tool stability. Sims *et al.*extended the semi-discretisation approach (developed by Stepan and Insperger[10;11]) to consider axial discretisation of the cutting tool. As a result, the variations in time delay could be accounted for within the model. The approach was then used by Yusoff and Sims[12] to optimise tool

geometry and perform experimental comparisons. More recently, Jin *et al.*[13] also explored the use of semi-discretisation methods. Dombovari and Stepan[14] further extended the semi-discretisation method by applying weighted distributed delays; a technique that allowed them to consider harmonically varying helix angles. Meanwhile, Khasawneh and Mann[15] developed a spectral element approach that could consider multiple delays in a generic configuration of time-delayed system. Finally, Compean *et al.*[16] applied the Enhanced Multistage Homotopy Perturbation Method to accommodate the multiple delays within a variable helix tool.

Despite this recent work, it is still difficult to properly understand the potential benefits of variable helix tool geometries, and to the author's knowledge there is a lack of experimental validation of the various modelling approaches that have been proposed. In the present study, an alternative variable helix model formulation is developed. Whilst this has some additional assumptions, it can provide a useful insight into the stability improvements by allowing the stability to be visualised using a filter frequency response function. Furthermore, the approach is hundreds of times faster computationally, compared to previous work by the author[8], which could enable better design and optimisation of the tool geometry.

The present work does not seek to provide new experimental analysis of variable helix tool stability. However, the potential modelling and validation challenges are explored by comparing the analytical stability predictions to well-established methods. First, fully-discrete and semi-discretised stability analysis approaches are compared to the new method. Second, time-domain simulations are used to illustrate the potential influence of non-linear cutting force coefficients. Consequently, this contribution illustrates possible reasons why variable-helix tools have more complex stability behaviour that is harder to predict, compared to regular tool geometries.

The remainder of the paper is organised as follows. First, the background theory (which can be found in many textbooks[1;17] is summarised for completeness. Then, the new modelling formulation is derived. A visual interpretation of the variable helix stability is presented, before describing the numerical approach used for stability analysis. Numerical and analytical stability results are then compared, in order to explore the significance of different modelling assumptions. Finally, following a discussion, some conclusions are drawn.

2 Theory

2.1 Classical milling dynamics

In the standard approach to modelling regenerative chatter[17] (Fig. 2), the total chip thickness h for tooth j at angle ϕ_j is given by:

$$h(\phi_j) = \left[s_t \sin\phi_j + (v_{j,0} - v_j)\right] g(\phi_j) \tag{1}$$

where $g(\phi_j)$ is a unit step function:

$$g(\phi_j) = \begin{cases} 1 & \leftarrow \quad \phi_{st} < \phi_j < \phi_{ex} \\ 0 & \leftarrow \quad \phi_j < \phi_{st} \text{ or } \phi_j > \phi_{ex} \end{cases} \tag{2}$$

This defines when the tool is engaged within the workpiece, i.e. within the angles ϕ_{st} and ϕ_{ex}. Meanwhile, $v_{j,0} - v_j$ is the difference between the previous and current instantaneous chip thickness.

Neglecting the quasi-static component $s_t \sin \phi_j$ in Eq. (1), and rewriting $v_{j,0} - v_j$ in terms of x and y coordinates gives

$$h(\phi_j) = [\Delta x \sin \phi_j + \Delta y \cos \phi_j]\, g(\phi_j) \tag{3}$$

where

$$\Delta x = x(t) - x(t - \tau) \tag{4}$$

$$\Delta y = y(t) - y(t - \tau) \tag{5}$$

Here, τ is the time delay between each tooth pass - with a variable helix tool the aim is to replace this with a distributed delay term that provides improved chatter stability. The cutting forces in the tangential and radial directions are given by:

$$\begin{aligned} f_{t,j} &= K_t a h(\phi_j) \\ f_{r,j} &= K_r f_{t,j} \end{aligned} \tag{6}$$

This assumes that the cutting forces are proportional to the instantaneous chip thickness. Some studies have suggested that this empirical approximation is inappropriate, and have instead proposed nonlinear

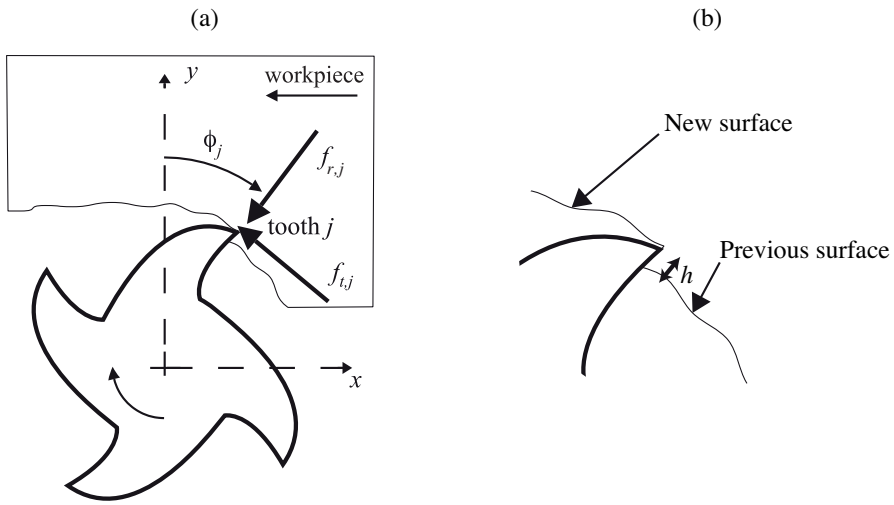

Figure 2. Milling model. (a) tool, workpiece, forces, and coordinate system; (b) close-up showing chip thickness h

(power-law) relationships[18]. This issue will be revisited later on, using a numerical time-domain model. However, for the present analysis a linear cutting force coefficient is assumed. Resolving the forces into the x and y directions, and summing for all the N_t teeth of the cutter gives:

$$\begin{aligned} f_x &= \sum_{j=1}^{N_t} -f_{t,j}\cos(\phi_j) - f_{r,j}\sin(\phi_j) \\ f_y &= \sum_{j=1}^{N_t} +f_{t,j}\sin(\phi_j) - f_{r,j}\cos(\phi_j) \end{aligned} \tag{7}$$

Further manipulation leads to:

$$\begin{aligned} f_x &= \frac{aK_t}{2}\sum_{j=1}^{N_t} a_{xx}\left[x(t)-x(t-\tau)\right] + a_{xy}\left[y(t)-y(t-\tau)\right]\} \\ f_y &= \frac{aK_t}{2}\sum_{j=1}^{N_t} a_{yx}\left[x(t)-x(t-\tau)\right] + a_{yy}\left[y(t)-y(t-\tau)\right]\} \end{aligned} \tag{8}$$

where the parameters $a_{xx}, a_{...}$ are the instantaneous direction factors, that relate the x and y-direction vibrations to the x and y-direction forces. They are given by[17]:

$$\begin{aligned} a_{xx} &= -g(\phi_j)\left[\sin(2\phi_j) + K_r(1-\cos(2\phi_j))\right] \\ a_{xy} &= -g(\phi_j)\left[1+\cos(2\phi_j) + K_r\sin(2\phi_j)\right] \\ a_{yx} &= +g(\phi_j)\left[1-\cos(2\phi_j) - K_r(\sin(2\phi_j))\right] \\ a_{yy} &= +g(\phi_j)\left[\sin(2\phi_j) - K_r(1+\cos(2\phi_j)\right] \end{aligned} \tag{9}$$

In their pioneering work, Budak and Altintas[19] considered the Fourier series expansion of these coefficients, and discussed the validity of neglecting all but the first term. This is equivalent to taking the average of each term over one tool revolution. For example, the term α_{xx}, corresponding to the time-averaged a_{xx} coefficient, is:

$$\alpha_{xx} = \frac{1}{2\pi}\int_0^{2\pi} -g(\phi_j)\left[\sin(2\phi_j) + K_r(1-\cos(2\phi_j))\right] d\phi_j \tag{10}$$

Here, the step function $g(\phi)$ can be removed and the limits of integration changed:

$$\alpha_{xx} = -\frac{1}{2\pi}\int_{\phi_{st}}^{\phi_{ex}} \sin(2\phi_j) + K_r(1-\cos(2\phi_j))d\phi_j \tag{11}$$

This can be repeated for a_{xy}, a_{yx}, a_{yy}, leading to:

$$\begin{aligned}
\alpha_{xx} &= \frac{1}{4\pi}\left[+\cos(2\phi_j) - 2K_r\phi_j + K_r\sin(2\phi_j)\right]_{\phi_{st}}^{\phi_{ex}} \\
\alpha_{xy} &= \frac{1}{4\pi}\left[-\sin(2\phi_j) - 2\phi_j + K_r\cos(2\phi_j)\right]_{\phi_{st}}^{\phi_{ex}} \\
\alpha_{yx} &= \frac{1}{4\pi}\left[-\sin(2\phi_j) + 2\phi_j + K_r\cos(2\phi_j)\right]_{\phi_{st}}^{\phi_{ex}} \\
\alpha_{yy} &= \frac{1}{4\pi}\left[-\cos(2\phi_j) - 2K_r\phi_j - K_r\sin(2\phi_j)\right]_{\phi_{st}}^{\phi_{ex}}
\end{aligned} \tag{12}$$

which (when the limits are evaluated) become independent of the tooth number j.

These equations form the basis of many stability analyses methods proposed in the literature. In the next section, the approach is revisited to consider the variable helix case. To simplify the analysis the case of vibrations in a single direction (the x-direction) are considered; the more general case of x and y-vibrations is given some thought in Section 7.

2.2 Variable helix formulation

In order to introduce the analysis method, consider a milling tool with two flutes, where the helix angle difference between the two flutes is α as shown in Fig. 3. Assume that the tool/workpiece system is flexible in the surface feed direction x, and completely rigid in the mutually perpendicular direction y. Define the tool rotation period as τ_r, and define the coefficient β as:

$$\beta = \frac{\tau_r \tan(\alpha)}{r_t 2\pi} \tag{13}$$

The cutting force in the x-direction is therefore:

$$f_x(t) = K_t \int_{a=0}^{a=b} a_{xx,1}(t)(x(t) - x(t - \tau_0 - \beta a)) + a_{xx,2}(t)(x(t) - x(t - \tau_0 + \beta a))da \tag{14}$$

where $a_{xx,i}$ is the time-periodic cutting force coefficient for the ith tooth. Accounting for this time-periodic behaviour allows the prediction of period-one and period-two instabilities[20;21]. Accounting for each tooth i individually enables the influence of the twisted flutes to be considered[22]. In this work, we neglect both of these effects and use the time-averaged cutting force coefficient, α_{xx}. This simplification gives:

$$f_x(t) = K_t\alpha_{xx} \int_{a=0}^{a=b} x(t) - x(t - \tau_0 - \beta a) + x(t) - x(t - \tau_0 + \beta a)da. \tag{15}$$

The continuous delay terms can now be rewritten using the Laplace transform:

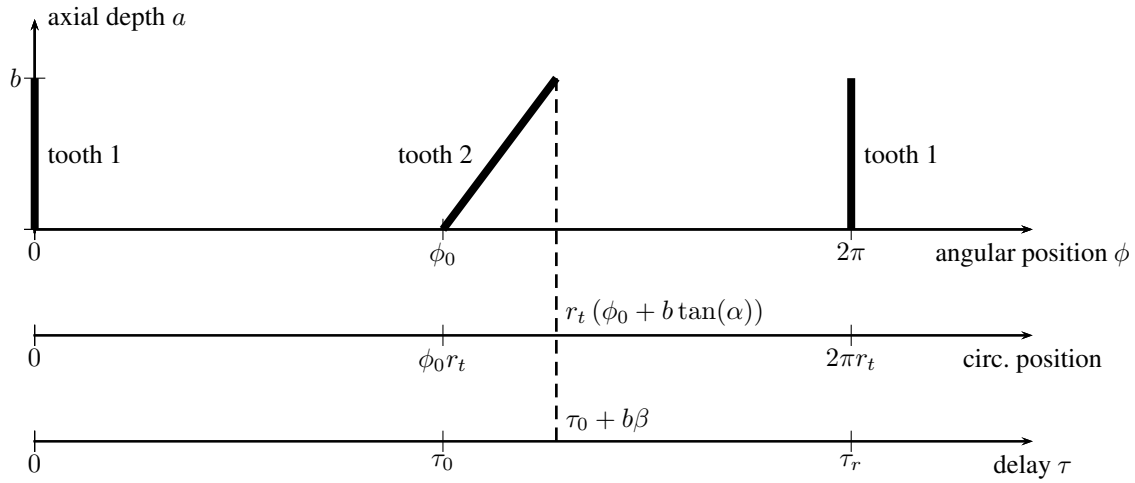

Figure 3. Schematic representation of a variable helix tool

$$\mathcal{L}(f_x(t)) = F_x(s) = \int_{t=0}^{t=\infty} e^{-st} K_t \alpha_{xx} \int_{a=0}^{a=b} x(t) - x(t - \tau_0 - \beta a) + x(t) - x(t - \tau_0 + \beta a) da dt. \quad (16)$$

Changing the order of integration leads to:

$$F_x(s) = K_t \alpha_{xx} \int_{a=0}^{a=b} \int_{t=0}^{t=\infty} e^{-st}(x(t) - x(t - \tau_0 - \beta a) + x(t) - x(t - \tau_0 + \beta a)) dt da. \quad (17)$$

Writing $\mathcal{L}(x(t))$ as $X(s)$ and applying the shift theorem gives:

$$F_x(s) = K_t \alpha_{xx} X(s) \int_{a=0}^{a=b} 2 - e^{-s(\tau_0 - \beta a)} - e^{-s(\tau_0 + \beta a)} da \quad (18)$$

which can finally be integrated with respect to a:

$$F_x(s) = K_t \alpha_{xx} X(s) \left[2a - \frac{e^{-s(\tau_0 - \beta a)}}{s\beta} + \frac{e^{-s(\tau_0 + \beta a)}}{s\beta} \right]_{a=0}^{a=b}. \quad (19)$$

Evaluating the limits of the integration leads to:

$$F_x(s) = K_t \alpha_{xx} X(s) \left(2b - \frac{e^{-s(\tau_0 - \beta b)}}{s\beta} + \frac{e^{-s(\tau_0 + \beta b)}}{s\beta} \right). \quad (20)$$

As an aside, it should be noted that the equivalent equation for a non-variable-helix tool can be obtained as:

$$\lim_{\beta \to 0} F_x(s) = K_t \alpha_{xx} X(s) b(2 - 2e^{-s\tau_0}) \quad (21)$$

which can be found in many textbooks, e.g.[1].

Eq. (20) allows the cutting process to be written as two transfer functions: a zero-order orientation and scaling coefficient, referred to as the *cutting gain*, G_c, and a delay term $G_d(s)$.

$$G_c = 2K_t\alpha_{xx}b \tag{22}$$

The delay transfer function for the variable helix tool is:

$$G_d(s) = 1 - \frac{e^{-s(\tau_0-\beta b)}}{2s\beta b} + \frac{e^{-s(\tau_0+\beta b)}}{2s\beta b} \tag{23}$$

whilst for a regular helix tool it becomes:

$$G_d(s) = 1 - e^{-s\tau_0}. \tag{24}$$

Eq. (24) is the transfer function for a rotating unit vector, as described by Tlusty[1], whilst Eq. (23) is the equivalent transfer function for a variable helix tool. To the author's knowledge, previous studies have not been able to obtain this transfer function for variable helix configurations. This is one contribution of the present study, and it should be reiterated that the key to the approach is the use of the Laplace transform and the shift theorem, in order to simplify the analysis of the continuous delays.

This paves the way for both (a) frequency domain solution of the variable helix stability problem; and (b) visual interpretation of the variable helix effect as a filter.

3 Visual interpretation for regular helix tools

A block-diagram representation of the regenerative chatter effect is shown in Fig. 4. Here, the system input R (which would ordinarily represent the forced vibration of the system) is set to zero, in order to perform a stability analysis of regenerative chatter. Assuming a harmonic response at frequency ω, and noting that Fig. 4 is a positive feedback system, the transfer function that governs the stability of the system is:

$$G_{tot}(j\omega) = -G_x(j\omega)G_d(j\omega)G_c \tag{25}$$

and from the Nyquist stability criterion

$$G_{tot}(j\omega) = -1 \tag{26}$$

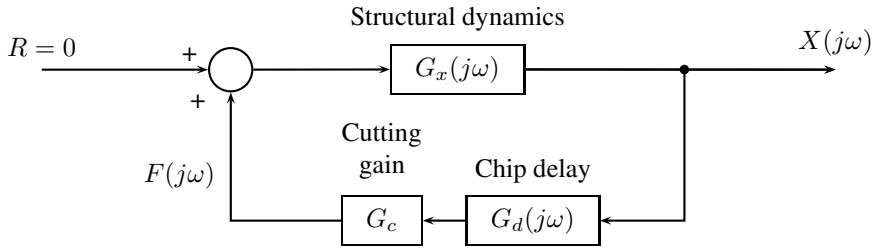

Figure 4. Block diagram for regenerative chatter instability

The consequence on stability is best explained using the bode diagrams depicted in Fig. 5, for the case of a regular helix tool (Eq. (24)). This approach is not new, but it is helpful to recap the concepts before extending them to the case of variable helix tools. In Fig. 5, Only the $G_x(j\omega)$ and $G_d(j\omega)$ transfer functions are shown, along with the total transfer function $G_{tot}(j\omega)$. The depth of cut is chosen arbitrarily as 1mm, and two spindle speeds are chosen.

At the stability boundary, the phase must be $-180°$ to partially satisfy Eq. (26). At these points the 'critical' frequency is denoted ω_c. The points are shown with solid markers on the bode diagrams. For each marker, the corresponding magnitude term can be used to determine the stability of the system, i.e. if $|G_{tot}(j\omega_c)| < 1$ (or < 0dB), then the system is stable.

In fact, for regular helix tools the magnitude response $|G_{tot}|$ is directly proportional to the depth of cut b, since b only appears in the cutting gain G_c. Consequently it is straightforward to compute the stability boundary directly as:

$$b_c = \frac{b}{|G_{tot}(j\omega_c)|} \tag{27}$$

These results are shown on Fig. 5e, along with a traditional stability lobe diagram. It can be seen that for each spindle speed there are multiple candidate chatter frequencies ω_c and that one of these candidates will govern the overall stability since it leads to the lowest possible value for b_c. Note that Fig. 5 only shows two potential chatter frequencies at each spindle speed, for clarity.

The behaviour at 1280 rpm (Fig. 5c&d) is particularly interesting because this demonstrates how aligning the tooth passing frequency with the natural frequency leads to increased stability. In other words, in Fig. 5c the delay transfer function has a very low magnitude, which reduces the overall

magnitude response G_{tot} at the natural frequency of the structure. This is well known in the machining dynamics literature, but not normally considered in the context of Bode diagram stability analysis.

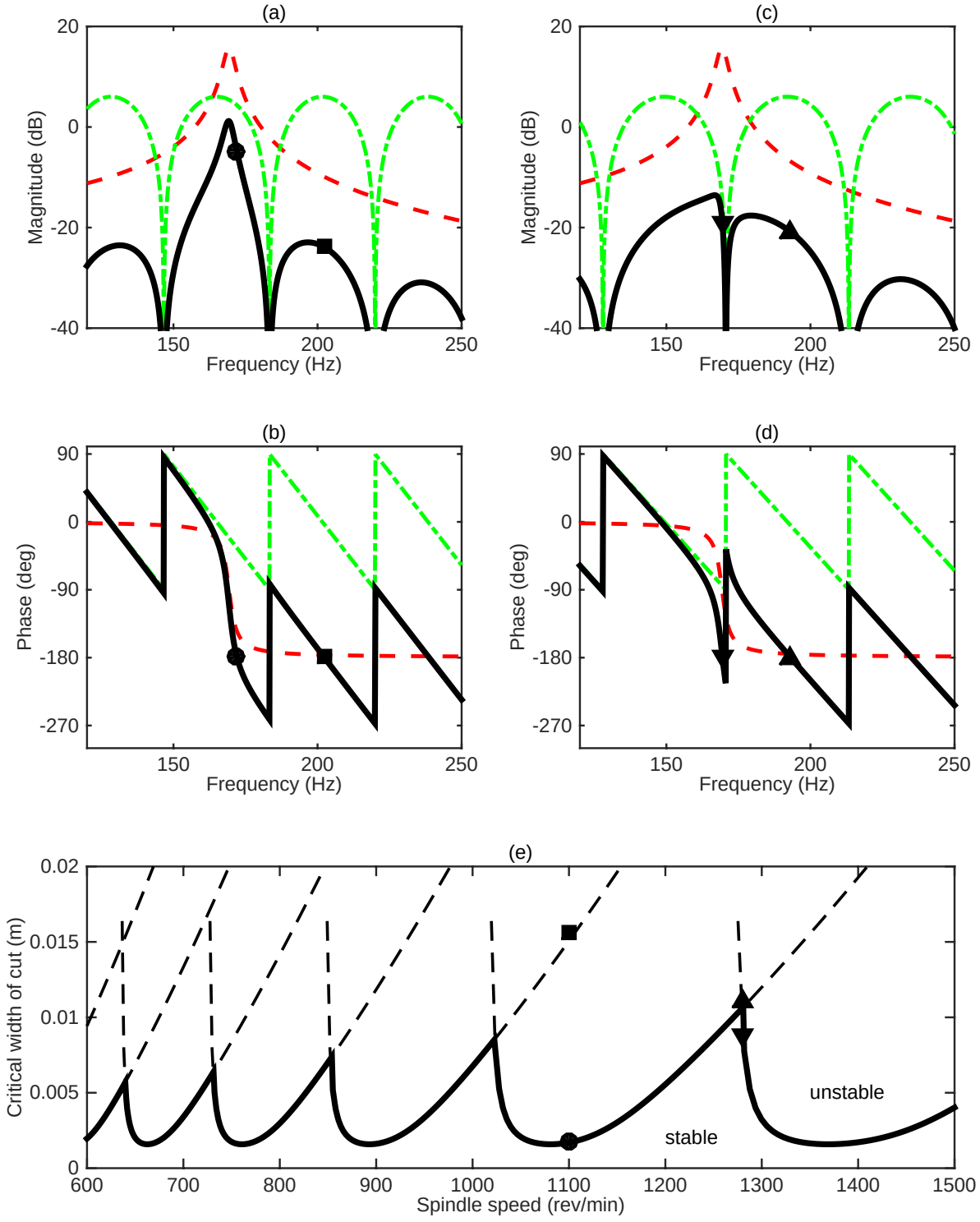

Figure 5. Schematic representation of stability analysis. (a) & (b) Bode diagram for $b = 1$mm, 1100 rpm; (c) & (d) Bode diagram for b=1mm, 1280 rpm. — — — Structure Transfer Function $G_x(j\omega)$ (mm/kN); — · — · — Delay transfer function $G_d(j\omega)$; ——— Negative feedback transfer function $G_{tot}(j\omega)$. Markers show the magnitude at critical frequencies where the phase is $-180°$. (e) Stability boundary. — — — boundary for each critical frequency; ——— overall stability boundary. Markers show the critical widths of cut corresponding to the scenarios in (a)-(d). Note that α_{xx} and G_c are negative for this example.

4 Visual interpretation for variable helix tools

Having summarised the Bode diagram stability analysis of regular helix tools, it is now possible to illustrate the implications of using a variable helix tool. To recap, the Laplace transform approach has shown that the difference between variable helix and regular helix tools can be entirely captured by the delay transfer functions shown in Equations 24 and 23. For regular helix it can be seen that the delay transfer function is a simple unit vector rotating around (1,0) on the Nyquist plane. This is reiterated in Fig. 6a; where the phase and amplitude responses are identical to those observed in Fig. 5, and the rotating unit vector is illustrated by the Nyquist plot. In Fig. 6, the frequency axes are non-dimensionalised by scaling by the tool rotation period τ_r. Low magnitude responses occur at dimensionless frequencies of 2,4,..., corresponding to the tooth passing frequencies. The transfer function is similar to a comb filter; in the previous section it was shown that the low amplitude frequencies can be harnessed to achieve high stability of the machining process.

For variable helix tools, the delay transfer function takes on a different form (Eq. (23)), which involves the depth of cut b. The transfer function frequency response is shown in Fig. 6b. As the depth of cut increases, the behaviour changes substantially compared to the comb filter observed in Fig. 6a. In particular, as the dimensionless frequency increases, the comb filter effect is diminished and the response tends toward unity. This could be shown more formally by inspection of Eq. (23). This behaviour is more pronounced for deeper depths of cut b. At intermediate dimensionless frequencies (e.g. 5-10) there are still regions of low-amplitude response, but the low amplitudes occur at different frequencies compared to the regular helix tool. On the Nyquist plane, the response appears as a spiral that winds towards the (1,0) coordinate as the frequency increases. This is in contrast to the regular helix behaviour, which exhibits a unit circle that continuously rotates around the (1,0) coordinate.

The behaviour illustrated in Fig. 6 can be directly interpreted to consider the implications for chatter stability and machining process design. This is in contrast to many previous studies on variable helix stability[8] which have not offered direct insight due to the numerical methods (e.g. eigenvalue analysis) employed. The most significant observation from Fig. 6b is that the response tends toward unity as the dimensionless frequency or depth of cut is increased. In contrast for a regular helix tool the magnitude will always alternate between 0 and 2, leading to strong patterns of stable (magnitude near 0) and unstable (magnitude near 2) behaviour as illustrated in Fig. 5. Meanwhile, the variable helix phase response tends towards zero, so that the delay transfer function has a very small influence on the total phase response.

Since this interpretation is a key feature of the present work, the approach is further illustrated in Fig. 7. Here, the analysis presented in Fig. 5a-b is repeated for a variable helix configuration. At low depths

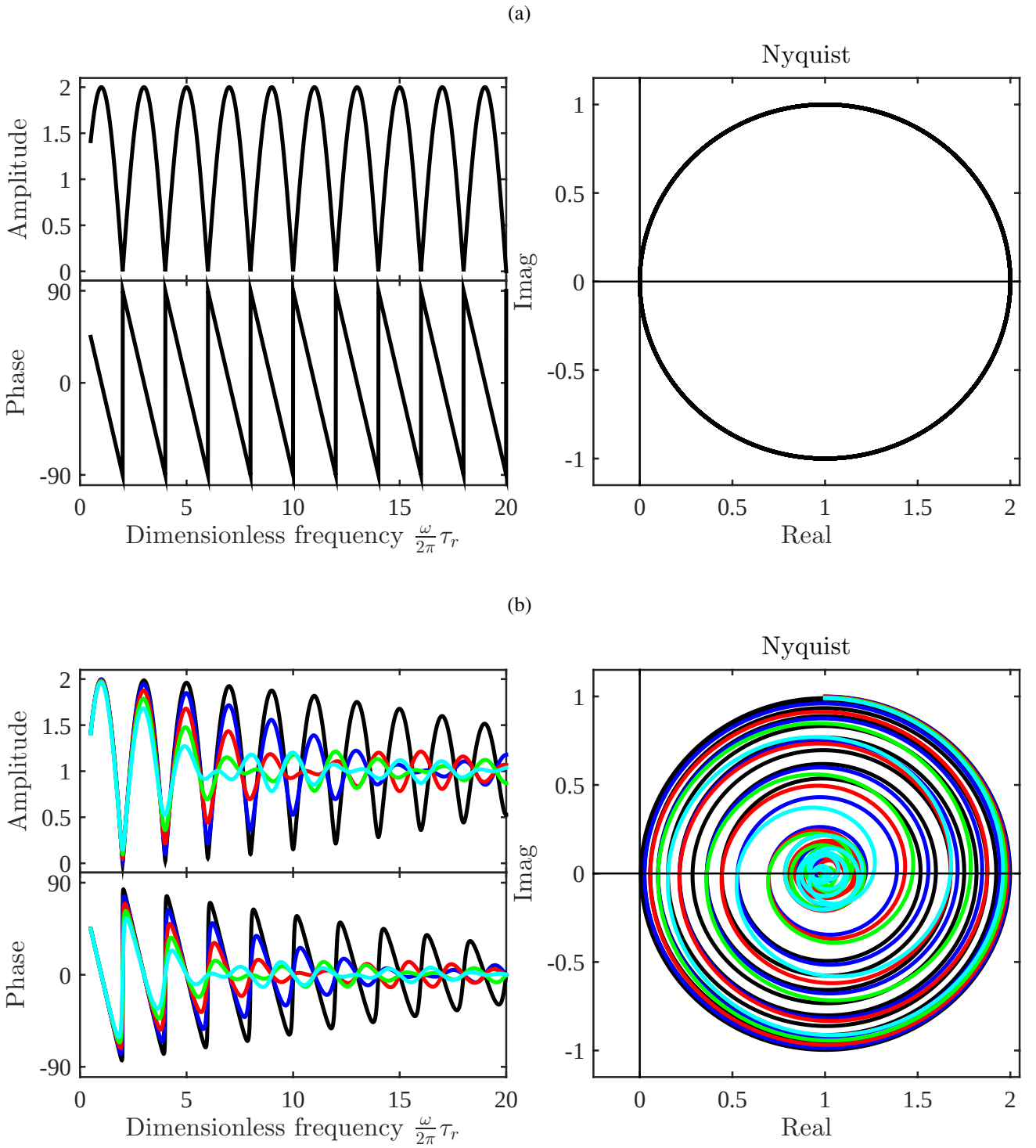

Figure 6. Chip transfer function. (a) regular helix tools, Eq. (24); (b) variable helix tool, Eq. (23), two flute tool with 25° helix angle difference, Black to cyan shows increasing depth of cut.

of cut (Fig. 7a-b) the behaviour is very similar to the regular helix case. There is some 'smoothing' of the delay transfer function, but the response is unstable as the magnitude is greater than 0dB at $\omega_c = 173$Hz. When the depth of cut is increased (Fig. 5c-d), the delay transfer function is substantially different. The comb filter effect is almost negligible, and so the overall transfer function G_{tot} is governed

by the structural dynamics and cutting gain. The system is stable, because the magnitude is less than 0dB for all critical frequencies ($\omega_c = 187, 244, ...$)Hz.

In Fig. 7e, the overall stability of the system is shown. This is obtained by repeating the bode diagram stability analysis for permutations of spindle speed and depth of cut. The two example results are shown superimposed. Finally, it is important to note that small ripples in the chip delay transfer function (Fig. 7d, green dashed line) can still have an influence on stability. In Fig. 7d the effect is to slightly increase the phase response near the structure's natural frequency. This has increased stability. However, at other spindle speeds the effect can be reversed, so that a critical frequency occurs close to the structure's natural frequency. This leads to islands of instability shown in Fig. 7e.

5 Implementation and validation

This section summarises the numerical procedures required for the new stability analysis method, and compares the results to alternative analysis methods.

The new method involves the following computational steps, which are straightforward to implement, as well as being computationally inexpensive:

1. Obtain the numerical frequency response function for the structural dynamics, $G_x(j\omega)$, from analysis or experiment.
2. Obtain the numerical value for the chip gain, G_c, from the cutting parameters of the system (Eq. (22)).
3. For each required spindle speed $\frac{60}{\tau_r}$ (revolutions per minute);
   (a) For each depth of cut b
      i. Evaluate $G_d(j\omega)$ numerically (Eq. (23)).
      ii. Combine with measured values of $G_x(j\omega)$ and G_c to obtain $G_{tot}(j\omega)$ (Eq. (25))
      iii. Identify frequencies ω_c where $\angle(G_{tot}(j\omega)) = -180°$.
      iv. Determine the corresponding value of $|G_{tot}(j\omega_c)|$.
      v. Choose the highest value of these $|G_{tot}(j\omega_c)|$.
      vi. If the gain is less than unity then the system is stable.

The solutions for this approach are now compared to those for the semi-discretisation method described by previous work[8]. The numerical parameters are summarised in Table 1, and these are chosen to be similar to Table 2 and Figure 14 in the previous study[8], although a higher spindle speed is considered in order to improve convergence of the semi-discretisation method, and to illustrate behaviour of interest.

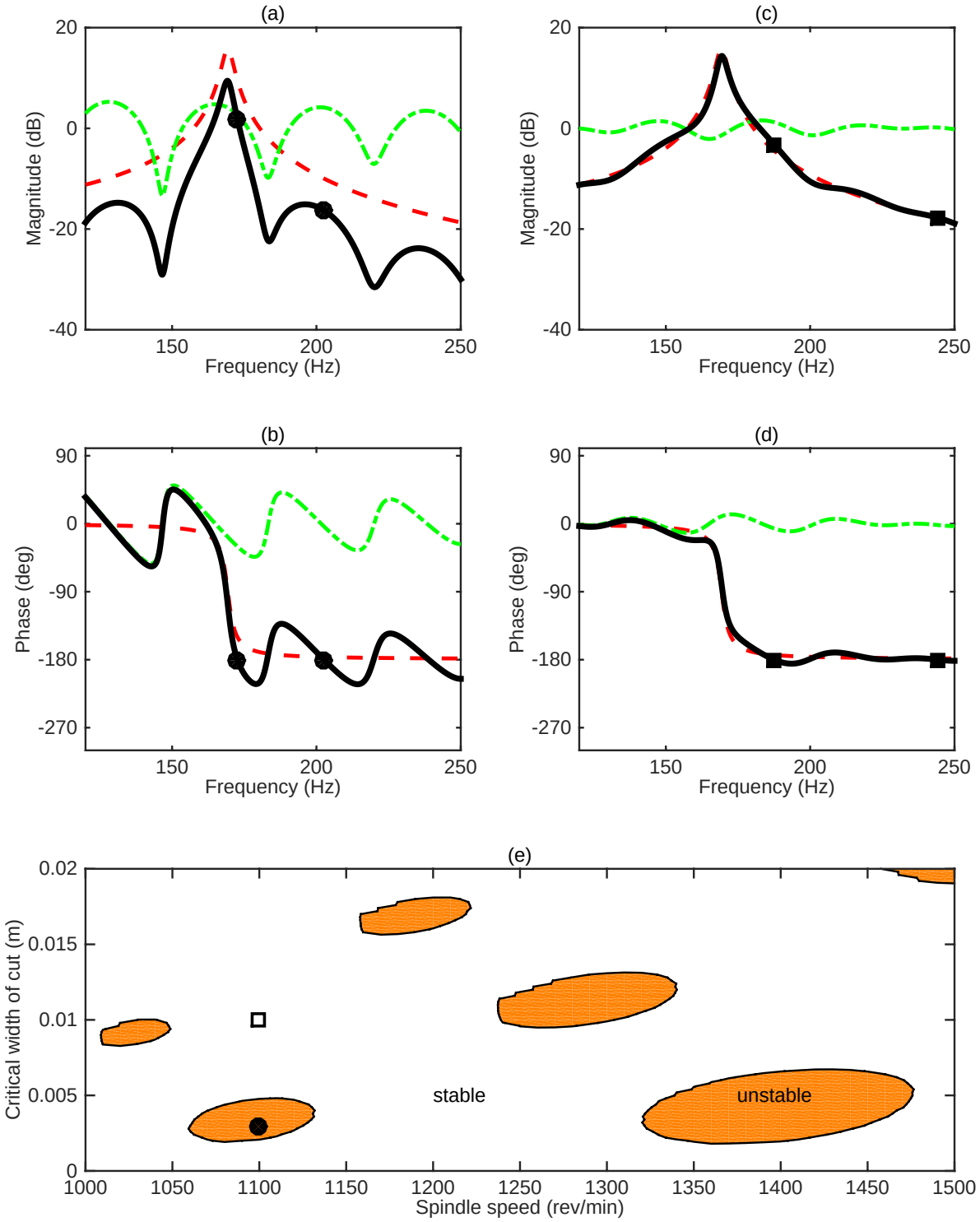

Figure 7. Schematic representation of stability analysis. (a) & (b) Bode diagram for $b = 3$mm, 1100 rpm; (c) & (d) Bode diagram for b=10mm, 1100 rpm. Structure Transfer Function $G_x(j\omega)$ (mm/kN); Delay transfer function $G_d(j\omega)$; Negative feedback transfer function $G_{tot}(j\omega)$. Markers show the locations of critical frequencies where the phase is $-180°$. (e) Overall chatter stability. Markers show stability boundaries obtained from the gain margins of (a) (•, unstable) and (c) (□, stable). Shading shows unstable regions.

The time-averaged semi-discretisation approach[8] was based upon the semi-discretisation method, but the cutting force coefficients were time-averaged, rather than accounting for their periodicity. Consequently, this method is most similar to the new Laplace approach presented in this work. The comparison is shown in Fig. 8a, and it can be seen that there is good agreement between the two methods.

parameter	value
modal mass (kg)	6.4363
modal natural frequency (Hz)	169.3090
modal damping ratio (-)	0.0112
cutting stiffness K_t (N/mm^2)	550
cutting stiffness K_r (-)	0.3636
tool radius (m)	0.0095
number of teeth	2
tooth pitch at tool tip	180°-180°
tool helix angle difference	25°
cutting radial immersion	full slot milling

Table 1. Numerical parameters for validation study.

The differences can be attributed to the numerical challenges associated with each method. In the new Laplace solution, the stability margin is calculated based upon discrete data points on the numerical frequency response function $G_{tot}(j\omega)$. Although the accuracy of this could be improved using linear interpolation, the present study simply used a nearest-neighbour data point. In the time-averaged semi-discretisation method, the accuracy of the stability boundary depends strongly on the discretisation step size. In the present study 400 discretisation points per tool revolution were used, leading to an eigenvalue problem of a similar order. Accuracy can be improved by increasing the number of discretisation points, but this can drastically increase the computational effort.

In Fig. 8b, the new method is compared to the semi-discretisation approach. The time-averaged semi-discretisation method took 75 minutes to solve on a desktop pc, whilst the new Laplace solution took just 22 seconds. However, it is clear that there are substantial differences between the time-averaged and multi-frequency methods at this range of spindle speeds.

This behaviour is explored in more detail by using a time-domain simulation, based upon the model described in previous work[23]. The model was computed for 100 simulated tool revolutions with 2048 time steps per revolution. Stability was determined by analysing the variance of once-per-revolution samples of the simulated vibration. For clarity, only the stable solutions are shown on Fig. 8b; it can be seen that these agree reasonably with the semi-discretisation solution at low spindle speeds (< 3000 rpm). At higher speeds the time-domain and semi-discretisation results differ from one-another: this could be due to differences in their convergence behaviour.

Further work is needed to investigate this behaviour in more detail, but given the close agreement between the two time-averaged methods (Fig. 8a) it is reasonable to conclude that the variable helix stability prediction is more susceptible to multi-frequency effects, compared to regular helix tools, for the parameter range considered.

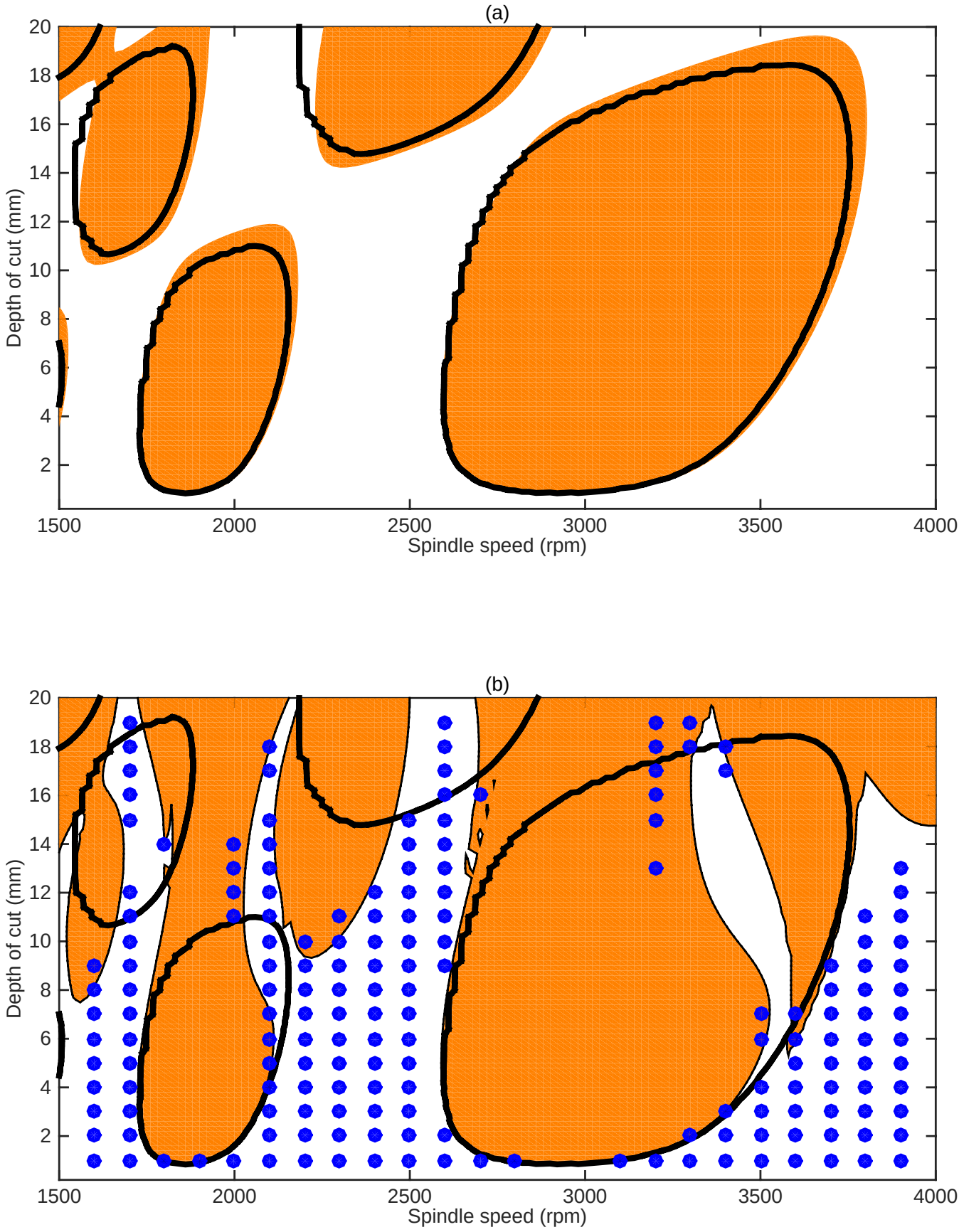

Figure 8. Validation against the semi-discretisation, fully discretised, and time domain methods. (a) New Laplace solution, Unstable discretised solution; (b) New Laplace solution, Unstable semi-discretisation solution; Stable linear simulation.

6 Influence of nonlinear cutting stiffness

The influence of nonlinear cutting force coefficients is less straightforward. In the present study, this phenomenon is demonstrated with the aid of a time-domain simulation, again based upon the model described in previous work[23]. Following Stepan[18], the cutting force coefficient is rewritten as

$$f_{t,j} = K_t K_1 a h(\phi_j)^{3/4}. \tag{28}$$

The new coefficient K_1 was chosen so that the linearised cutting force coefficient is unchanged at the mean chip thickness. The time domain results are compared to the Laplace solution, and the semi-discretisation solution, in Fig. 9. It can be seen that there are significant differences between the three results. This also suggests that the variable helix stability prediction is susceptible to un-modelled effects such as nonlinear cutting stiffness, compared to the behaviour of regular helix tools.

However, it should be noted that for the non-linear scenario it is not straightforward to compare time-domain simulations with analytical stability methods. For example, the analytical methods imply linearisation around an operating condition (e.g. the mean chip thickness used for Eq. (28)), and the nonlinearity may cause sensitivity to the choice of initial conditions.

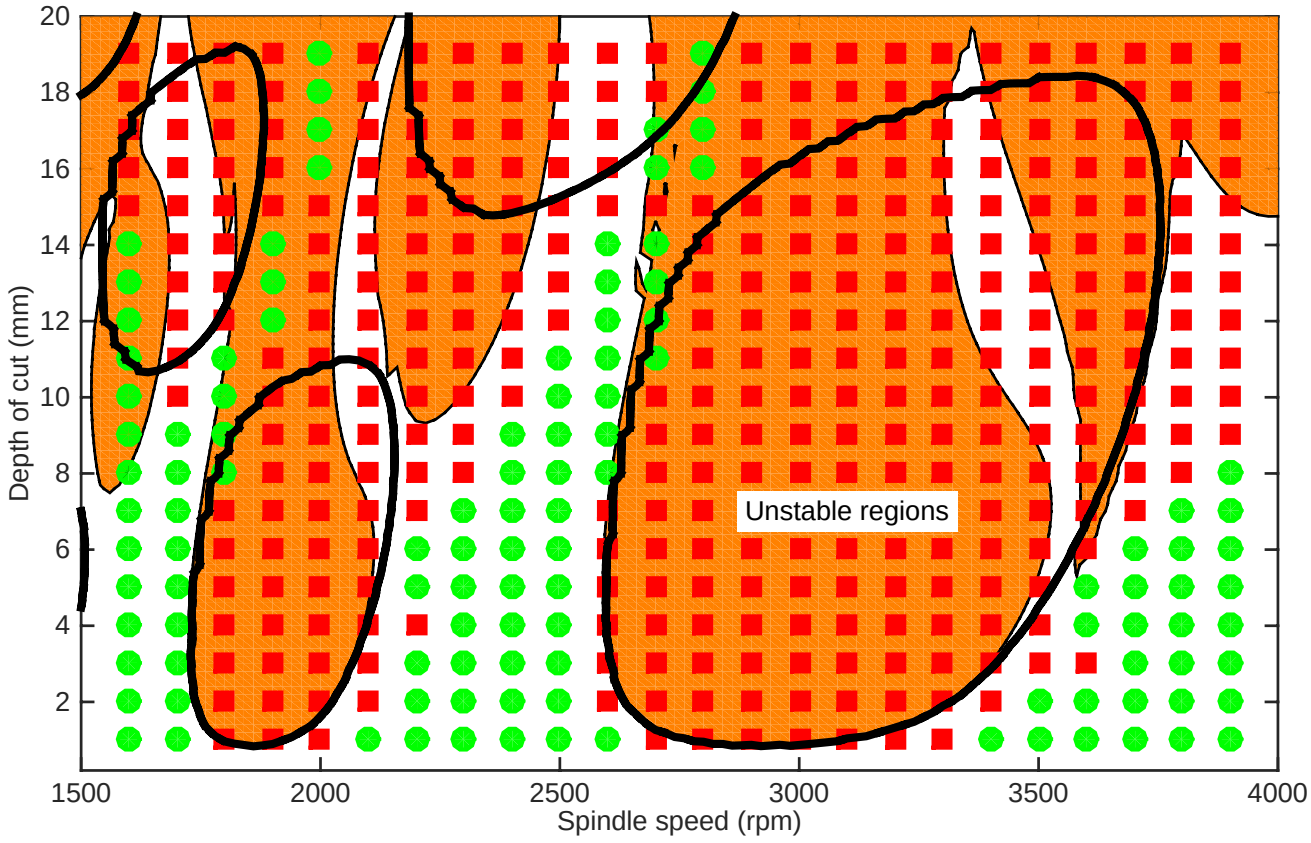

Figure 9. Validation against the semi-discretisation, fully discretised, and nonlinear time domain methods. Laplace solution; Stable nonlinear simulation; Unstable nonlinear simulation; Unstable multi-frequency solution.

7 Discussion

Before drawing conclusions, a number of points are worthy of further discussion.

7.1 Two-direction formulation

One drawback with the approach presented here is that the formulation has only been presented for vibrations in a single degree of freedom. However, the main focus of the present study was to offer a new means of visualising variable helix stability, and to illustrate some of the inaccuracies that can occur when well-established assumptions are used for the special case of variable helix tools. The points have been illustrated without resorting to the more cumbersome formulations needed for vibrations in x and y directions. Despite this, it is useful to briefly consider whether, and how, the new Laplace approach could be extended to the two-direction formulation.

Returning to Eq. (14), it is clear that for the two-direction case there will be two simultaneous equations, describing forces in the x and y directions, and coupling introduced by the a_{xy} and a_{yx} coefficients (Eq. (9)). Time averaging of these coefficients will lead to corresponding simultaneous equations replacing Eq. (15). Now, the Laplace transform can be applied separately to each of the terms in the simultaneous equations, because the transform is linear and follows the principal of superposition. Continuing with this approach will lead to the coupling terms being collected in a 2×2 matrix of gains $\mathbf{G_c}$, along with a scalar transfer function $G_d(j\omega)$.

In order to perform a stability analysis, the multi-input-multi-output coupled system can be transformed into two uncoupled single-input-single-output systems. In the general case this requires an eigenvalue solution for each frequency ω_c, but since the system is 2×2, the solution can be achieved analytically.

Consequently, it seems feasible that the approach can be extended to the case of mutually perpendicular vibrations with a relative straightforward development of the approach, and only a small increase in computational cost. This should certainly be considered for further work, but in practice the need for further experimental validation of behaviour is probably a more urgent step.

7.2 Multi-frequency formulation

An alternative to the time-averaged approach is to consider the Fourier series expansion of the direction factors shown in Eq. (12). In this case, a frequency domain solution could be achieved by following the detailed methodology described by Wereley[24]. However, in this case the stability analysis becomes much more cumbersome, as the formulation is likely to involve higher-order matrices of transfer

functions. It remains to be seen whether this approach would offer any advantages compared to the semi-discretisation method, in terms of computational cost or visualisation/design aids.

7.3 Other helix geometries

A final concern with the new Laplace approach is the assumption that the helix angles are constant for each tooth. This can be overcome in two ways. First, it could be possible to rewrite Eq. (16) to describe other geometries in an analytical fashion. An example would be sinusoidal variations in the tool delay. However, solving this analytically is probably not possible and so Eq. (19) could not be written using such an approach. The alternative approach is to consider the helix angles as piecewise constant. In this case, it should be possible to write Eq. (19) as a summation of terms, leading to a more complicated but otherwise useful expression for $G_d(j\omega)$.

7.4 Role of structural damping

Before drawing conclusions, it is useful to consider one nuance of the bode diagrams presented in Fig. 7. The examples suggest that at higher depths of cut the critical frequencies are more sensitive to the phase of the structural dynamics $G_x(j\omega)$, because the variation in the delay transfer function $G_d(j\omega)$ is smaller. This raises the question of whether variable helix tools are more likely to benefit from damping, compared to regular helix tools. This damping could be in the form of structural damping (inherent, or intentionally added), or un-modelled damping mechanisms (such as process damping[25;26]). Further work could explore this experimentally.

8 Conclusions

In this contribution, a new formulation for predicting the chatter stability of variable helix tools has been described. The following conclusions can be drawn:

1. The Laplace formulation provides new insight into the stability of variable helix tools as it allows the distributed delay parameters to be visualised as a filter. This can be contrasted with the comb filter effect that is well-known for regular helix tools.
2. The formulation is compatible with numerical frequency response function data, and consequently does not require modal models to represent the structural dynamics of the system. This offers some convenience compared to previous formulations. In addition, the new formulation is hundreds of times faster than some other methods for variable helix stability analysis. Consequently the approach is potentially convenient for industrial application.

3. A major issue with the formulation is that the stability prediction appears to be highly sensitive to the un-modelled effects of nonlinear cutting stiffness. In addition, the time-averaging of the cutting force coefficients appears to have a dramatic effect on the stability. Both of these issues have been illustrated on a specific scenario. Further work is needed to explore the relevance of these on practical machining problems.

9 Acknowledgements

The author is grateful for the constructive comments made by both reviewers. In addition, Dr T Baldacchino kindly proof-read the nomenclature and equations in the draft manuscript. This research received no specific grant from any funding agency in the public, commercial, or not-for-profit sectors.

References

1. Tlusty J. *Manufacturing Processes and Equipment*. New Jersey: Prentice Hall, 1999.
2. Chung B, Smith S and Tlusty J. Active damping of structural modes in high speed machine tools. *Journal of Vibration and Control* 1997; 3(3): 279–295.
3. Tarng Y, Kao J and Lee E. Chatter suppression in turning operations with a tuned vibration absorber. *Journal of Materials Processing Technology* 2000; 105(1): 55–60.
4. Sims N. Vibration absorbers for chatter suppression: A new analytical tuning methodology. *Journal of Sound and Vibration* 2007; 301(3-5): 592–607. DOI:10.1016/j.jsv.2006.10.020. URL http://www.scopus.com/inward/record.url?eid=2-s2.0-33846429613&partnerID=40&md5=4d2c6898f1f5cd4630
5. Seguy S, Insperger T, Arnaud L et al. On the stability of high-speed milling with spindle speed variation. *International Journal of Advanced Manufacturing Technology* 2010; 48(9-12): 883–895. URL http://www.scopus.com/inward/record.url?eid=2-s2.0-77953608906&partnerID=40&md5=8c9eda0ef6a9c0746a
6. Stone BJ. The effect on the chatter behaviour of cutters with different helix angles on adjacent teeth. *Advances in Machine Tool Design and Research, Proc of 11th International MTDR Conference University of Birmingham* 1970; A: 169–180.
7. Budak E. An analytical design method for milling cutters with non-constant pitch to increase stability, part 1: Theory and part 2: Application. *Journal of Manufacturing Science and Engineering* 2003; 125: 29–38. URL http://www.scopus.com/scopus/inward/record.url?eid=2-s2.0-0039335175&partnerID=40&rel=R6.0.0.
8. Sims N, Mann B and Huyanan S. Analytical prediction of chatter stability for variable pitch and variable helix milling tools. *Journal of Sound and Vibration* 2008; 317(3-5): 664–686. DOI:10.1016/j.jsv.2008.03.045.
9. Turner S, Merdol D, Altintas Y et al. Modelling of the stability of variable helix end mills. *International Journal of Machine Tools and Manufacture* 2007; 47(9): 1410–1416.
10. Insperger T and Stepan G. Updated semi-discretization method for periodic delay-differential equations with discrete delay. *International Journal for Numerical Methods in Engineering* 2004; 61(1): 117.
11. Insperger T and Stépán G. *Semi-discretization for time-delay systems: stability and engineering applications*, volume 178. Springer Science & Business Media, 2011.

12. Yusoff A and Sims N. Optimisation of variable helix tool geometry for regenerative chatter mitigation. *International Journal of Machine Tools and Manufacture* 2011; 51(2): 133–141. URL http://www.scopus.com/inward/record.url?eid=2-s2.0-78650713355&partnerID=40&md5=cf8e0a0b69371b5f15

13. Jin G, Zhang Q, Hao S et al. Stability prediction of milling process with variable pitch and variable helix cutters. *Proceedings of the Institution of Mechanical Engineers, Part C: Journal of Mechanical Engineering Science* 2014; 228(2): 281–293. DOI:10.1177/0954406213486381. URL http://pic.sagepub.com/content/228/2/281.abstract. http://pic.sagepub.com/content/228/2/281.full.pdf+html.

14. Dombovari Z and Stepan G. The effect of helix angle variation on milling stability. *Journal of Manufacturing Science and Engineering, Transactions of the ASME* 2012; 134(5). URL http://www.scopus.com/inward/record.url?eid=2-s2.0-84867019429&partnerID=40&md5=c88c058cd1bd53804c

15. Khasawneh F and Mann B. A spectral element approach for the stability analysis of time-periodic delay equations with multiple delays. *Communications in Nonlinear Science and Numerical Simulation* 2013; 18(8): 2129–2141. URL http://www.scopus.com/inward/record.url?eid=2-s2.0-84875254350&partnerID=40&md5=e99f261ad402b03e91

16. Compean F, Olvera D, Campa F et al. Characterization and stability analysis of a multivariable milling tool by the enhanced multistage homotopy perturbation method. *International Journal of Machine Tools and Manufacture* 2012; 57: 27–33.

17. Altintas Y. *Manufacturing Automation: Metal Cutting Mechanics, Machine Tool Vibrations, and CNC Design*. Cambridge University Press, 2000.

18. Stepan G. Modelling nonlinear regenerative effects in metal cutting. *Philosophical Transactions of the Royal Society of London, Part A* 2001; 359: 739–757.

19. Budak E and Altintas Y. Analytical prediction of chatter stability in milling - part i: general formulation. *Journal of Dynamic Systems, Measurement and Control* 1998; 120: 22–30.

20. Merdol SD and Altintas Y. Multi frequency solution of chatter stability for low immersion milling. *Journal of Manufacturing Science and Engineering, Transactions of the ASME* 2004; 126(3): 459–466.

21. Insperger T, Stepan G, Bayly PV et al. Multiple chatter frequencies in milling processes. *Journal of Sound and Vibration* 2003; 262(2): 333–345.

22. Khasawneh F, Bobrenkov O, Mann B et al. Investigation of period-doubling islands in milling with simultaneously engaged helical flutes. *Journal of Vibration and Acoustics, Transactions of the ASME* 2012; 134(2). URL http://www.scopus.com/inward/record.url?eid=2-s2.0-84856013830&partnerID=40&md5=5f406cffc8b8efdf4e

23. Sims N. The self-excitation damping ratio: a chatter criterion for time-domain milling simulations. *Journal of Manufacturing Science and Engineering* 2005; 127(3): 433–445.

24. Wereley N. *Analysis and control of time periodic systems*. PhD Thesis, Massachusetss Institute of Technology, 1991.

25. Sims N and Turner M. The influence of feed rate on process damping in milling: Modelling and experiments. *Proceedings of the Institution of Mechanical Engineers, Part B: Journal of Engineering Manufacture* 2011; 225(6): 799–810. URL http://www.scopus.com/inward/record.url?eid=2-s2.0-80051862668&partnerID=40&md5=cf7f08a563caed7f73

26. Budak E and Tunc LT. A new method for identification and modeling of process damping in machining. *Journal of Manufacturing Science and Engineering* 2009; 131(5): 051019–10.